Applied Energy Symposium 2019: Low carbon cities and urban energy systems
October 16-18, 2019, Xiamen, China
Paper ID: 0198

OPERATION OPTIMIZATION OF URBAN MULTI-ENERGY SYSTEMS CONSIDERING CHARGING ROUTES IN THE TRANSPORTATION NETWORK: A MIXIED USER EQUILIBRIUM METHOD

Shiwei Xie[1], Jieyun Zheng[2], Jueying Wang[1], Zhijian Hu[1], Linyao Zhang[2], Zhi Chen[1]

1 School of Electrical Engineering and Automation, Wuhan University, Wuhan City, Hubei Province, China
2 Economic and Technological Research Institute of State Grid Fujian Electric Power Co., Ltd, Fuzhou, China

ABSTRACT

To meet and adapt to the increasing multiple energy demands, smart city has become the trend of the urban development. Based on this background, an operation optimization framework of urban multi-energy systems is proposed, where the power distribution network, natural gas network and transportation network are coupled by integrated energy stations. With the aim of minimizing operation costs, the model optimizes the operation strategies of renewable energy generation, combined heat and power, gas boiler, power to gas, electric chiller, absorption chiller and fast charging facilities coordinately. This model considers the traffic assignment problem for both non-electric and electric vehicles in the transportation network. Due to the advanced communication technologies, the optimal routes (with minimum travel expense) for both traveling and charging can be identified and provided for all drivers, and this routing behavior would lead to the traffic equilibrium state. To describe the steady state distribution of traffic flow, a mixed user equilibrium model is established, where the route selections for non-electric vehicle and charging navigations for electric vehicle are incorporated. To solve the proposed nonlinear model, convex relaxation is performed. Finally, the simulation results illustrate the effectiveness of the proposed model.

Keywords: electric vehicle, multi-energy system, transportation network, mixed user equilibrium

NONMENCLATURE

Notations *(omitting subscripts and superscripts)*	
p , q	Active power / reactive power
g , π	Natural gas flow / pressure
f , x	Traffic flow on path / link
t , u	Travel time / Minimal travel time
U , I	The magnitude of voltage / current
C, η	Operation cost / Conversion coefficient
G	Gas flow bound value
P, Q	Active / Reactive power bound value
Ω	Sets of available node or line
K, Λ	Sets of traffic path / O-D demand
Subscripts and superscripts	
EV/N-EV	Electric vehicle / Non-electric vehicle
EB/EL	Electric bus/line
GS/GC/GN/GP	Gas source/compressor/node/pipeline
TS	Transformer substation
TL	Transportation link
Other Parameters	
Δ	Duration time (1 hour)
R_{ij}, X_{ij}	Resistance / Reactance
Φ_{ij}	Gas pipeline transmission factor
β^{Cur}	Maximum curtailment rate
$\bar{C}_a^{\mathrm{TL}}$	Road capacity

1. INTRODUCTION

Nowadays, the multi-energy system (MES) is becoming a promising concept to improve energy efficiency in urban area [1]. The operation framework for the MES usually relies on integrated energy station (IES) [2], which couples the power distribution networks (PDN) and natural gas network (GN). However, due to the widespread utilization of electric vehicles (EVs) [3], the inspired emerging trend of smart city that jointly considers the transportation and energy systems is now entailing the systematic methodologies to model the operation of this new-type system. Although some research endeavor to model the operation issues in PDNs [4], in GNs [5], in MESs [6], and in transportation network (TN) [7] independently, the operation model considering the integration of them has not been reported yet.

To fill this research gap, the structure of urban MES

Selection and peer-review under responsibility of the scientific committee of CUE2019

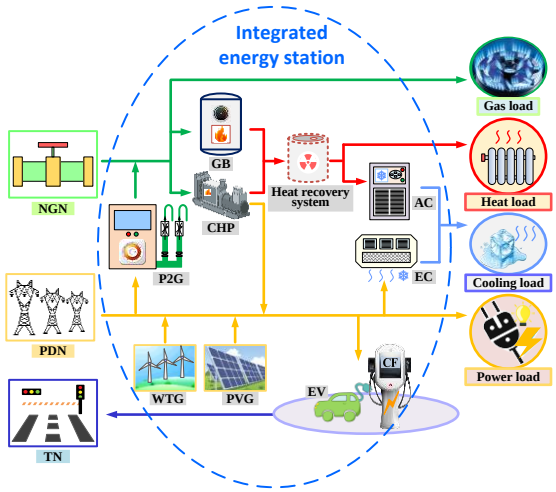

Fig 1 Structure of urban mulit-energy system

considering the integration of transportation network (TN) is proposed originally in this paper, as shown in Fig 1. In such a framework, the PDN, GN and TN are coupled by the IES that serves gas, heat, cooling and power energy demand simultaneously. To perform energy exchange, smart devices including renewable distributed generators (DGs), combined heat and power (CHP), gas boiler (GB), power to gas (P2G), electric chiller (EC), absorption chiller (AC) and fast charging facilities (CFs) are considered to be installed in the IES. It is worth noting that the fast CFs can be regarded as bridge that joins the PDN and TN, therefore the charging route can affect the operational strategies of the MES. On this basis, the main task of this paper is to model the operation optimization problem for such an MES considering the EV charging routes. To describe the driving patterns, a mixed user equilibrium (UE) is applied. Then the model formulation is developed with its convex relaxation method. Finally, case studies verify the effectiveness of the approach.

2. TRANSPORTATION NETWORK MODEL CONSIDERING THE CHARGING ROUTES

2.1 The model of charging link

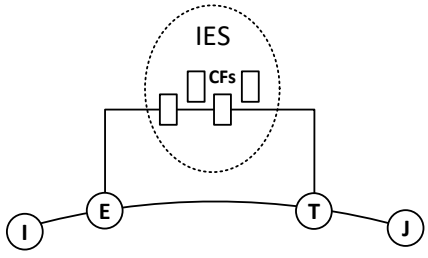

Fig 2 Representation of a charging link passing an IES

A novel charging link model based on the IES is proposed in this section. The fast CFs are located in an IES that is beside a road link. In order to facilitate building the mathematical TN model, the charging route connecting to CFs (in an IES) can be represented a five-nodes five-link module, shown in Fig 2. If a link I-J is beside an IES, it would allow the EVs to get charged in the station. Thus, it includes two paths: I-E-T-J (normal link) and I-E-IES-T-J (charging link). It is suitable to assume that the travel time on bypass link E-T is zero since it is very short, and the original travel time of link I-J ($t_{IJ} = T_0$) will be distributed into two link (I-E and T-J), for example, $t_{IE} = T_0/2$, $t_{ET} = 0$, $t_{TJ} = T_0/2$. Then, the travel time of EVs on charging link consists of the time on link I-E and T-J, and the charging time (T_C) on the station (i.e., $t_C^{\mathrm{EV}} = t_{IE} + T_C + t_{TJ}$). If an EV is in need of charging, its travel route would include a charging link. Other vehicles without needing battery recharge would seek their route that excludes the charging link. They are both allowed to be informed with the travel information by center management system, and selects their best route with the shortest travel time, thereby reaching their respective UE state.

2.2 The mixed UE modeling

The UE state is usually applied to describe traffic flow patterns in actual application. As is described in [3], the traffic flow will reach a UE if the vehicle's travel time on all active paths between any give O-D pair are the same, and less than those on any unused paths. Considering the EVs and non-EVs, a mixed UE state can be expressed as a logic form [7]:

$$\left\{\begin{array}{l}\text{if } f_{rs,k,t}^{\mathrm{EV}} > 0, \text{ then } t_{rs,k,t}^{\mathrm{EV}} = u_{rs,t}^{\mathrm{EV}}, \\ \text{if } f_{rs,k,t}^{\mathrm{EV}} = 0, \text{ then } t_{rs,k,t}^{\mathrm{EV}} \geq u_{rs,t}^{\mathrm{EV}},\end{array}\right\}, \forall (r,s), \forall k, \forall t \quad (1)$$

$$\left\{\begin{array}{l}\text{if } f_{rs,k,t}^{\text{N-EV}} > 0, \text{ then } t_{rs,k,t}^{\text{N-EV}} = u_{rs,t}^{\text{N-EV}}, \\ \text{if } f_{rs,k,t}^{\text{N-EV}} = 0, \text{ then } t_{rs,k,t}^{\text{N-EV}} \geq u_{rs,t}^{\text{N-EV}},\end{array}\right\}, \forall (r,s), \forall k, \forall t \quad (2)$$

where superscript 'EV' and 'N-EV' are used to represent the vehicles that needing and not needing to be recharged. $f_{rs,k,t}^{\mathrm{EV}}$ and $f_{rs,k,t}^{\text{N-EV}}$ are the traffic flow on path k between (r,s). $t_{rs,k,t}^{\mathrm{EV}}$ and $t_{rs,k,t}^{\text{N-EV}}$ are the travel expense (time) on path k. $u_{rs,t}^{\mathrm{EV}}$ and $u_{rs,t}^{\text{N-EV}}$ are the minimal travel cost between each O-D pair (r,s). By introducing two auxiliary variables, $v_{rs,k,t}^{\mathrm{EV}}$ and $v_{rs,k,t}^{\text{N-EV}}$, constraints (1) and (2) can be mathematically expressed as follows.

$$\left\{\begin{array}{l}0 \leq f_{rs,k,t}^{\mathrm{EV}} \leq \mathrm{M} \cdot (1 - v_{rs,k,t}^{\mathrm{EV}}) \\ 0 \leq t_{rs,k,t}^{\mathrm{EV}} - u_{rs,t}^{\mathrm{EV}} \leq \mathrm{M} \cdot v_{rs,k,t}^{\mathrm{EV}}\end{array}\right\}, \forall (r,s), \forall k, \forall t \quad (3)$$

$$\left\{\begin{array}{l}0 \leq f_{rs,k,t}^{\text{N-EV}} \leq \mathrm{M} \cdot (1 - v_{rs,k,t}^{\text{N-EV}}) \\ 0 \leq t_{rs,k,t}^{\text{N-EV}} - u_{rs,t}^{\text{N-EV}} \leq \mathrm{M} \cdot v_{rs,k,t}^{\text{N-EV}}\end{array}\right\}, \forall (r,s), \forall k, \forall t \quad (4)$$

where M is a big constant. It's worth noting that these UE constraints constitute the KKT conditions of a well-know traffic assignment problem (TAP). As described in [3], the

UE state can be satisfied when the KKT condition is included in the transportation optimization model.

3. MULTI-ENERGY SYSTEM MODEL FORMULATION

Based on the framework introduced above, fast CFs are located in the IES, and thus couples the TN and PDN. Considering the interdependencies between networks, the objective and related constraint of the coordinated operation optimization model are presented as follows.

3.1 Objective function

The objective is composed of the operation costs in the PDN, GN, TN and IESs, which is shown as follows.

$$F^{\mathrm{MES}} = f_{\mathrm{ope}}^{\mathrm{PDN}} + f_{\mathrm{ope}}^{\mathrm{GN}} + f_{\mathrm{ope}}^{\mathrm{TN}} + f_{\mathrm{ope}}^{\mathrm{IES}} \tag{5}$$

$$\begin{aligned} f_{\mathrm{ope}}^{\mathrm{PDN}} = &\sum_t \Delta \sum_{ij\in\Omega^{\mathrm{EL}}} \mathrm{C}^{\mathrm{Loss}} \hat{I}_{ij,t} \mathrm{R}_{ij} + \sum_t \Delta \sum_{j\in\Omega^{\mathrm{DG}}} \mathrm{C}^{\mathrm{Cur\_DG}} p_{j,t}^{\mathrm{Cur\_DG}} \\ &+ \sum_t \Delta \sum_{j\in\Omega^{\mathrm{DG}}} \mathrm{C}^{\mathrm{DG}} p_{j,t}^{\mathrm{DG}} + \sum_t \Delta \sum_{j\in\Omega^{\mathrm{TS}}} \mathrm{C}^{\mathrm{TS}} p_{j,t}^{\mathrm{TS}} \end{aligned} \tag{6}$$

$$f_{\mathrm{ope}}^{\mathrm{GN}} = \sum_t \Delta \sum_{j\in\Omega^{\mathrm{GS}}} \mathrm{C}^{\mathrm{S}} g_{j,t}^{\mathrm{S}} \tag{7}$$

$$f_{\mathrm{ope}}^{\mathrm{TN}} = \sum_t \sum_{a\in\Omega^{\mathrm{TL\text{-}R}}} \zeta' \cdot t_{a,t} x_{a,t} + \sum_t \sum_{a\in\Omega^{\mathrm{TL\text{-}E}}} \zeta'' \cdot T_C \cdot x_{a,t} \tag{8}$$

$$\begin{aligned} f_{\mathrm{ope}}^{\mathrm{IES}} = &\sum_t \sum_{j\in\mathrm{IES}} \Delta \cdot \mathrm{C}^{\mathrm{GB}} g_{j,t}^{\mathrm{GB}} + \sum_t \sum_{j\in\mathrm{IES}} \Delta \cdot \mathrm{C}^{\mathrm{CHP}} g_{j,t}^{\mathrm{CHP}} \\ &+ \sum_t \sum_{j\in\mathrm{IES}} \Delta \cdot \mathrm{C}^{\mathrm{P2G}} p_{j,t}^{\mathrm{P2G}} + \sum_t \sum_{j\in\mathrm{IES}} \Delta \cdot \mathrm{C}^{\mathrm{EC}} p_{j,t}^{\mathrm{EC}} \\ &+ \sum_t \sum_{j\in\mathrm{IES}} \Delta \cdot \mathrm{C}^{\mathrm{AC}} p_{j,t}^{\mathrm{AC}} \end{aligned} \tag{9}$$

In (6), the operation cost in PDN includes the energy loss, DG curtailment, and energy production. The gas supply cost is given in (7). In TN, the travel expense is mainly associated with the travel time (ζ') and charging cost (ζ''), shown in (8). The related costs in IES (mainly maintenance cost) are given in (9), where the operation of CBs, CHPs, P2Gs, ECs and ACs are considered.

3.2 Operation constraints

The constraints regarding to the system operation in the PDN, GN and TN are formulated below.

Cons-PDN:

1) Power flow equation

$$\begin{aligned} \sum_{jk\in\mathrm{JK}(j)} p_{jk,t} = &\sum_{ij\in\mathrm{IJ}(j)} p_{ij,t} - \sum_{ij\in\mathrm{IJ}(j)} \hat{I}_{ij,t} \mathrm{R}_{ij} \\ &- p_{j,t}^{\mathrm{L}} + p_{j,t}^{\mathrm{TS}}, \forall j \in \Omega^{\mathrm{EB}}, \forall t \end{aligned} \tag{10}$$

$$\begin{aligned} \sum_{jk\in\mathrm{JK}(j)} q_{jk,t} = &\sum_{ij\in\mathrm{IJ}(j)} q_{ij,t} - \sum_{ij\in\mathrm{IJ}(j)} \hat{I}_{ij,t} \mathrm{X}_{ij} \\ &- q_{j,t}^{\mathrm{L}} + q_{j,t}^{\mathrm{TS}}, \forall j \in \Omega^{\mathrm{EB}}, \forall t \end{aligned} \tag{11}$$

$$\begin{aligned} \hat{U}_{j,t} = &\hat{U}_{i,t} - 2(p_{ij,t}\mathrm{R}_{ij} + q_{ij,t}\mathrm{X}_{ij}) \\ &+ \hat{I}_{ij,t}(\mathrm{R}_{ij}^2 + \mathrm{X}_{ij}^2), \forall ij \in \Omega^{\mathrm{EL}}, \forall t \end{aligned} \tag{12}$$

$$\hat{U}_{i,t}\hat{I}_{ij,t} = p_{ij,t}^2 + q_{ij,t}^2, \forall ij \in \Omega^{\mathrm{EL}}, \forall t \tag{13}$$

In (10)-(13), the branch flow equations [8] are used to describe the power flow. In order to avoid the quadratic terms, we use $\hat{U}_{j,t}$ and $\hat{I}_{ij,t}$ as substitutes for voltage and current (i.e., $\hat{U}_{j,t} = U_{j,t}^2$ and $\hat{I}_{ij,t} = I_{ij,t}^2$). It should be noted that we distinguish the equations in the PDN and the IES. As introduced above, the integration of DGs is considered in the IES (refer to equation (35)), which is not included in (10)-(11).

2) Security constraint

$$0 \le \hat{I}_{ij,t} \le \overline{\mathrm{I}}^2, \forall ij \in \Omega^{\mathrm{EL}}, \forall t \tag{14}$$

$$\underline{\mathrm{U}}^2 \le \hat{U}_{j,t} \le \overline{\mathrm{U}}^2, \forall j \in \Omega^{\mathrm{EB}}, \forall t \tag{15}$$

$$\underline{\mathrm{P}}_j^{\mathrm{TS}} \le p_{j,t}^{\mathrm{TS}} \le \overline{\mathrm{P}}_j^{\mathrm{TS}}, \forall j \in \Omega^{\mathrm{TS}}, \forall t \tag{16}$$

$$\underline{\mathrm{Q}}_j^{\mathrm{TS}} \le q_{j,t}^{\mathrm{TS}} \le \overline{\mathrm{Q}}_j^{\mathrm{TS}}, \forall j \in \Omega^{\mathrm{TS}}, \forall t \tag{17}$$

3) Distributed energy generation

$$(1-\beta^{\mathrm{Cur}})\mathrm{P}_{j,t}^{\mathrm{DG}} \le \tilde{p}_{j,t}^{\mathrm{DG}} \le \mathrm{P}_{j,t}^{\mathrm{DG}}, \forall j \in \Omega^{\mathrm{DG}}, \forall t \tag{18}$$

$$(1-\beta^{\mathrm{Cur}})Q_{j,t}^{\mathrm{DG}} \le \tilde{q}_{j,t}^{\mathrm{DG}} \le Q_{j,t}^{\mathrm{DG}}, \forall j \in \Omega^{\mathrm{DG}}, \forall t \tag{19}$$

Two types of renewable energy source (wind and solar energy) are considered for DGs. As shown in (18)-(19), the active power curtailment for DGs is allowed within a certain range.

Cons-GN:

1) Gas source

$$\underline{G}_{j,t}^{\mathrm{S}} \le g_{j,t}^{\mathrm{S}} \le \overline{G}_{j,t}^{\mathrm{S}}, \forall j \in \Omega^{\mathrm{GS}}, \forall t \tag{20}$$

2) Gas pressure limit

$$\underline{\pi}_j \le \pi_{j,t} \le \overline{\pi}_j, \forall j \in \Omega^{\mathrm{GN}}, \forall t \tag{21}$$

3) Gas pipeline capacity

$$\underline{\mathrm{G}}_{ij,t} \le g_{ij,t} \le \overline{\mathrm{G}}_{ij,t}, \forall ij \in \Omega^{\mathrm{GP}}, \forall t \tag{22}$$

4) Gas flow equation

$$\sum_{jk\in\mathrm{JK}(j)} g_{jk,t} = \sum_{ij\in\mathrm{IJ}(j)} g_{ij,t} + g_{j,t}^{\mathrm{S}} - g_{j,t}^{\mathrm{L}}, \forall j \in \Omega^{\mathrm{GN}}, \forall t \tag{23}$$

$$\mathrm{sgn}(\pi_{i,t}^2, \pi_{j,t}^2) g_{ij,t}^2 = \Phi_{ij}(\pi_{i,t}^2 - \pi_{j,t}^2), \forall ij \in \Omega^{\mathrm{GP}}, \forall t \tag{24}$$

5) Gas compressor

$$\pi_{i,t} = \Phi_{ij}\pi_{j,t}, \forall ij \in \Omega^{\mathrm{GC}}, \forall t \tag{25}$$

$$\underline{\mathrm{G}}_{ij,t}^{\mathrm{C}} \le g_{ij,t}^{\mathrm{C}} \le \overline{\mathrm{G}}_{ij,t}^{\mathrm{C}}, \forall ij \in \Omega^{\mathrm{GC}}, \forall t \tag{26}$$

In the GN, gas source supply is limited by (20). Expressions (21) and (22) set the bounds on gas pressure and flow, respectively. Gas flow balance is formulated by (23), which imposes that the sum of gas inflows of a node is equal to the sum of gas outflows at any moment. The amount of gas flow through a pipeline can be expressed by Weymouth equation [1], as shown in (24). The operation constraint of gas compressors is characterized by (25)-(26), where the output pressure is a multiple of input pressure.

Cons-TN:

$$t_{a,t}(x_{a,t}) = t_{a,t}^{0}\left[1+0.15\left(x_{a,t}/\bar{\mathrm{C}}_{a}^{\mathrm{TL}}\right)^{4}\right], \forall a \in \Omega^{\mathrm{TL}}, \forall t \quad (27)$$

$$\begin{aligned} x_{a,t} = & \sum_{rs\in\Lambda^{\mathrm{OD}}}\sum_{k\in \mathrm{K}_{rs}^{\mathrm{EV}}} f_{rs,k,t}^{\mathrm{EV}}\delta_{rs,k,a}^{\mathrm{EV}} \\ & + \sum_{rs\in\Lambda^{\mathrm{OD}}}\sum_{k\in \mathrm{K}_{rs}^{\mathrm{N\text{-}EV}}} f_{rs,k,t}^{\mathrm{N\text{-}EV}}\delta_{rs,k,a}^{\mathrm{N\text{-}EV}}, \forall a \in \Omega^{\mathrm{TL}}, \forall t \end{aligned} \quad (28)$$

$$\sum\nolimits_{k\in \mathrm{K}_{rs}^{\mathrm{EV}}} f_{rs,k,t}^{\mathrm{EV}} = \tau_{rs,t}^{\mathrm{EV}}, \forall rs \in \Lambda^{\mathrm{OD}}, \forall t \quad (29)$$

$$f_{rs,k,t}^{\mathrm{EV}} \geq 0, \forall rs \in \Lambda^{\mathrm{OD}}, \forall k \in \mathrm{K}_{rs}^{\mathrm{EV}}, \forall t \quad (30)$$

$$\sum\nolimits_{k\in \mathrm{K}_{rs}^{\mathrm{N\text{-}EV}}} f_{rs,k,t}^{\mathrm{N\text{-}EV}} = \tau_{rs,t}^{\mathrm{N\text{-}EV}}, \forall rs \in \Lambda^{\mathrm{OD}}, \forall t \quad (31)$$

$$f_{rs,k,t}^{\mathrm{N\text{-}EV}} \geq 0, \forall rs \in \Lambda^{\mathrm{OD}}, \forall k \in \mathrm{K}_{rs}^{\mathrm{N\text{-}EV}}, \forall t \quad (32)$$

$$\begin{cases} 0 \leq f_{rs,k,t}^{\mathrm{EV}} \leq \mathrm{M}\cdot(1-v_{rs,k,t}^{\mathrm{EV}}) \\ 0 \leq t_{rs,k,t}^{\mathrm{EV}} - u_{rs,t}^{\mathrm{EV}} \leq \mathrm{M}\cdot v_{rs,k,t}^{\mathrm{EV}} \\ \forall rs \in \Lambda^{\mathrm{OD}}, \forall k \in \mathrm{K}_{rs}^{\mathrm{EV}}, \forall t \end{cases} \quad (33)$$

$$\begin{cases} 0 \leq f_{rs,k,\omega}^{\mathrm{N\text{-}EV}} \leq \mathrm{M}(1-v_{rs,k,\omega}^{\mathrm{N\text{-}EV}}) \\ 0 \leq t_{rs,k,\omega}^{\mathrm{N\text{-}EV}} - u_{rs,\omega}^{\mathrm{N\text{-}EV}} \leq \mathrm{M}\cdot v_{rs,k,\omega}^{\mathrm{N\text{-}EV}} \\ \forall rs \in \Lambda^{\mathrm{OD}}, \forall k \in \mathrm{K}_{rs}^{\mathrm{N\text{-}EV}}, \forall t \end{cases} \quad (34)$$

From the above, the traffic operation considering the UE of both EV and NEV can be constrained by (27)-(34).

Cons-IES:

1) Energy balance constraints

$$\begin{aligned} \sum_{jk\in \mathrm{JK}(j)} p_{jk,t} = & \sum_{ij\in \mathrm{IJ}(j)} p_{ij,t} - \sum_{ij\in \mathrm{IJ}(j)} I_{ij,t}^{2}\mathrm{R}_{ij} - \sum_{a\in C(j)} \eta\cdot x_{a,t} \\ & - p_{j,t}^{\mathrm{L}} - p_{j,t}^{\mathrm{P2G}} - p_{j,t}^{\mathrm{EC}} + p_{j,t}^{\mathrm{CHP}}, \forall j \in \Omega^{\mathrm{IES}}, \forall t \end{aligned} \quad (35)$$

$$\begin{aligned} \sum_{jk\in \mathrm{JK}(j)} g_{jk,t} = & \sum_{ij\in \mathrm{IJ}(j)} g_{ij,t} - g_{j,t}^{\mathrm{L}} - g_{j,t}^{\mathrm{CHP}} \\ & - g_{j,t}^{\mathrm{GB}} + g_{j,t}^{\mathrm{P2G}}, \forall j \in \Omega^{\mathrm{IES}}, \forall t \end{aligned} \quad (36)$$

$$p_{j,t}^{\mathrm{h\_CHP}} + p_{j,t}^{\mathrm{h\_GB}} + p_{j,t}^{\mathrm{h\_HE}} = p_{j,t}^{\mathrm{h\_L}} + p_{j,t}^{\mathrm{h\_AC}}, \forall j \in \Omega^{\mathrm{IES}}, \forall t \quad (37)$$

$$p_{j,t}^{\mathrm{c\_EC}} + p_{j,t}^{\mathrm{c\_AC}} = p_{j,t}^{\mathrm{c\_L}}, \forall j \in \Omega^{\mathrm{IES}}, \forall t \quad (38)$$

Equations (35)-(38) represent the electric power, gas, hot and cool energy balance in the IES, respectively. Comparing (31) with (6), EV charging demand, P2G and EC power requirement, as well as the power injection obtained from CHP are integrated in an IES bus. The expression (32) implies that the CHP (or CB) can convert natural gas into heat energy, while the P2G consumes the electrical power and produces natural gas energy. Similarly, equations (33) and (34) characterize the hot and cool balance of supply and demand, which relies on the related conversion devices including CHP, GB, HE, AC and EC in the IES.

2) Energy conversion constraints

$$g_{j,t}^{\mathrm{P2G}} = \frac{3.412\, p_{j,t}^{\mathrm{P2G}}\times\eta^{\mathrm{P2G}}}{\mathrm{GHV}}, \forall j \in \Omega^{\mathrm{IES}}, \forall t \quad (39)$$

$$p_{j,t}^{\mathrm{CHP}} = \frac{\mathrm{GHV}\times g_{j,t}^{\mathrm{CHP}}\times\eta_{\mathrm{GE}}^{\mathrm{CHP}}}{3.412}, \forall j \in \Omega^{\mathrm{IES}}, \forall t \quad (40)$$

$$p_{j,t}^{\mathrm{h\_CHP}} = \frac{g_{j,t}^{\mathrm{CHP}}\times\eta_{\mathrm{GH}}^{\mathrm{CHP}}\times\mathrm{GHV}}{3.412}, \forall j \in \Omega^{\mathrm{IES}}, \forall t \quad (41)$$

$$p_{j,t}^{\mathrm{h\_GB}} = \frac{g_{j,t}^{\mathrm{GB}}\times\eta^{\mathrm{GB}}\times\mathrm{GHV}}{3.412}, \forall j \in \Omega^{\mathrm{IES}}, \forall t \quad (42)$$

$$p_{j,t}^{\mathrm{c\_EC}} = p_{j,t}^{\mathrm{EC}}\times\eta^{\mathrm{EC}}, \forall j \in \Omega^{\mathrm{IES}}, \forall t \quad (43)$$

$$p_{j,t}^{\mathrm{c\_AC}} = p_{j,t}^{\mathrm{h\_AC}}\times\eta^{\mathrm{AC}}, \forall j \in \Omega^{\mathrm{IES}}, \forall t \quad (44)$$

The amount of natural gas produced by P2G can be computed by (39), where GHV is gross heating value. It can be noted that the unit of GHV is BTU/m³, and coefficient 3.412 is to convert 'W' to 'BTU/h'. Analogously, (40)-(42) are the energy conversion (BTU/h to W) expressions for CHP and GB, and (43)-(44) are that for EC and AC.

3.3 Convex relaxation

Since the integer variables have been introduced in the model inevitably (e.g., $v_{rs,k,t}^{\mathrm{EV}}, v_{rs,k,t}^{\mathrm{N\text{-}EV}}$), the proposed model formulation is a mixed-integer nonlinear program. To solve the problem, convex relaxation is conducted.

By applying conic relaxation method, equation (9) can be reformulated as follows:

$$\left\| 2P_{ij,t} \;\; 2Q_{ij,t} \;\; \hat{I}_{ij,t} - \hat{U}_{i,t} \right\|_2^{\mathrm{T}} \leq \tilde{I}_{ij,t} + \hat{U}_{i,t}, \forall ij \in \Omega^{\mathrm{EL}}, \forall t \quad (45)$$

In (45), conic relaxation is performed by replacing "=" with "≤" and its solution could be exact enough [9].

To solve the nonlinear expression (20), equivalent transformation can be firstly made in (aa), where $\hat{\pi}_{i,t}$ is the square of the pressure.

$$\mathrm{sgn}(\hat{\pi}_{i,t},\hat{\pi}_{j,t})g_{ij,t}^{2} = g_{ij,t}\left|g_{ij,t}\right| = \Phi_{ij}(\hat{\pi}_{i,t}-\hat{\pi}_{j,t}), \forall ij, \forall t \quad (46)$$

Following with the way adopted in [1], a modified piecewise linearization method can be used to relax equation (46), shown as follows:

$$\begin{cases} Y(g_n) = g_n\,|\,g_n\,|, n = 0,1,\cdots,\bar{n} \\ g_{ij,t} = g_0 + \sum_{n=1}^{\bar{n}}(g_n - g_{n-1})\cdot\delta_{ij,n,t} \\ \Phi_{ij}(\hat{\pi}_{i,t}-\hat{\pi}_{j,t}) = Y(g_0) + \sum_{n=1}^{\bar{n}}[Y(g_n)-Y(g_{n-1})]\cdot\delta_{ij,n,t} \\ \delta_{ij,n+1,t} \leq m_{ij,n,t} \leq \delta_{ij,n,t}, 0 \leq \delta_{ij,n,t} \leq 1, m_{ij,n,t} \in \{0,1\} \end{cases} \quad (47)$$

where $\delta_{ij,n,t}$ and $m_{ij,n,t}$ are two auxiliary variables to indicate the interval of the optimal solution. It can be noted that the above approach is also suitable for the non-convex traffic time function (23). Similarly, the reformulated linearized constraints can be provided as:

$$\begin{cases} Y'(x_n) = t_{a,t}^{0}\left[1+0.15\cdot(x_n/\bar{\mathrm{C}}_{a}^{\mathrm{TL}})^{4}\right], n = 0,1,\cdots,\bar{n} \\ x_{a,t} = x_0 + \sum_{n=1}^{\bar{n}}(x_n - x_{n-1})\cdot\delta'_{a,n,t} \\ t_{a,t} = Y'(x_n) + \sum_{n=1}^{\bar{n}}[Y'(x_n)-Y'(x_n)]\cdot\delta'_{a,n,t} \\ \delta'_{a,n+1,t} \leq m'_{a,n,t} \leq \delta'_{a,n,t}, 0 \leq \delta'_{a,n,t} \leq 1, m_{a,n,t} \in \{0,1\} \end{cases} \quad (48)$$

Therefore, the mixed-integer linear model can be represented as follows:

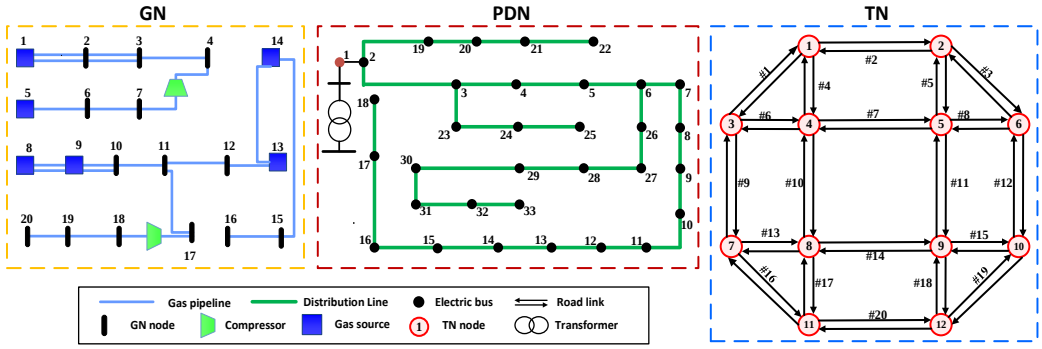

Fig 3 The schematic of three coupled test systems: GN, PDN and TN.

$$\begin{cases} \min F^{\mathrm{MES}} = f_{\mathrm{ope}}^{\mathrm{PDN}} + f_{\mathrm{ope}}^{\mathrm{GN}} + f_{\mathrm{ope}}^{\mathrm{TN}} + f_{\mathrm{ope}}^{\mathrm{IES}} \\ \text{s.t. Cons-PDN*:}\{(10)\text{-}(12),(14)\text{-}(19),(45)\} \\ \quad \text{Cons-GN*:}\{(20)\text{-}(23),(25)\text{-}(26),(47)\} \\ \quad \text{Cons-TN*:}\{(28)\text{-}(34),(48)\} \\ \quad \text{Cons-IES*:}\{(35)\text{-}(44)\} \end{cases} \tag{49}$$

4. CASE STUDIES

This section presents the numerical results based on a 20-node GN [1], 33-bus PDN [9] and 12-node TN [3]. The topology and related information are shown in Fig. 3. Four IESs are considered and the related data are given in Table 1. It is also assumed that the maximum allowable active/reactive power limit for lines is 0.5/0.4 (in p.u. with a base power value of 10 MVA if it is not particularly mentioned). Voltage and current data are given by $\bar{U}$=1.06, $\underline{U}$=0.94, and $\bar{I}$=2. At the slack bus 1, the supply capacity of transformer is 1.2 and the reference voltage is 1.0. The unit travel and charging cost are set as ζ'=2 \$/min and ζ''=3 \$/min. The cost coefficients in objective and energy conversion efficiency are provided in Table x. The GHV of natural gas is 40611 BTU/m^3. The maximum power curtailment rates of DGs (β) are set to 30%. Three seasonal typical days representing summer, intermediate and winter are used to test the operation problem, shown in Fig 4. The proposed model is programed in MATLAB and solved by calling CPLEX.

Table 1 Data of the IESs

No.	Bus number	Gas node	Road Link	Hot demand	Cool demand	Installed Devices
1	5	6	#2	17.07	17.19	WTG(3MW) PVG(3MW) GB(440SCM) CHP(380SCM) P2G(6MW) EC(9MW) AC(5MW)
2	11	9	#9	23.15	15.52	
3	16	16	#12	19.54	14.68	
4	26	20	#20	15.68	13.91	

Table 2 Cost coefficient and conversion efficiency

C^{Loss}	0.3 \$/kWh	η^{P2G}	58%
C^{TS} / $C^{\mathrm{Cur\_DG}}$	0.4 \$/kWh	$\eta_{\mathrm{GE}}^{\mathrm{CHP}}$	51%
C^{W}	0.23 \$/MBtu	$\eta_{\mathrm{GH}}^{\mathrm{CHP}}$	62%
C^{GB}	0.01 \$/MBtu	η^{GB}	93%
C^{CHP}	0.04 \$/MBtu	η^{EC}	52%
C^{P2G} / C^{EC} / C^{AC}	0.08 \$/kWh	η^{AC}	88%

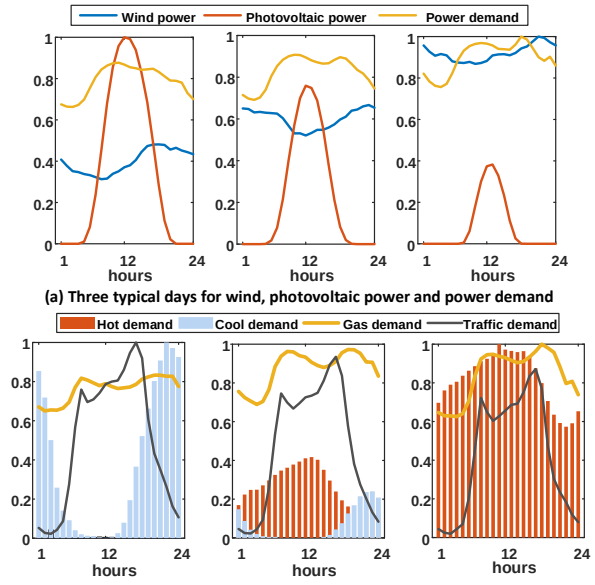

Fig 4 Three typical seasonal days (in p.u)

Table 3 The results of operation costs

	$f_{\mathrm{ope}}^{\mathrm{PDN}}$	$f_{\mathrm{ope}}^{\mathrm{GN}}$	$f_{\mathrm{ope}}^{\mathrm{TN}}$	$f_{\mathrm{ope}}^{\mathrm{IES}}$	F^{MES}
Cost/ \$	18731.9	98213.3	29877.3	286649.4	433471.9

Table 3 shows the optimal results of operation costs. It can be seen that the operation cost in the IESs is much greater, indicating the importance of considering the full energy conversion in the station. To make more observations, the energy balance in the station No.1 is given in Figs 5-7. The operation strategies for heat energy balance in Fig 5 show that hot demand is firstly satisfied by the GBs, while the CHPs produce heat energy during the peak periods (i.e., the third typical day). In Fig 6, the cooling demand is supported mainly by the ECs and ACs especially for the first day (summer). By considering the EV charging demand that is affected by traffic flow patterns, the demand for electricity will increase, as shown in Fig 7. With the integration of renewable energy sources, the power demand is mainly supplied by DGs

inside the IES, and the insufficient parts are purchased from the main grid.

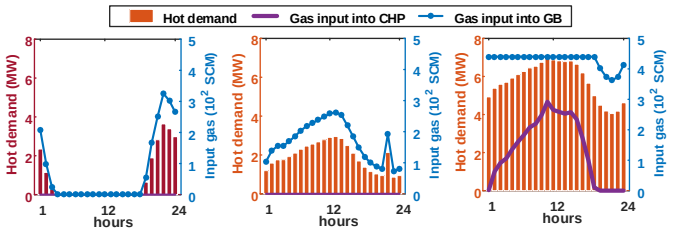

Fig 5 Heat energy balance

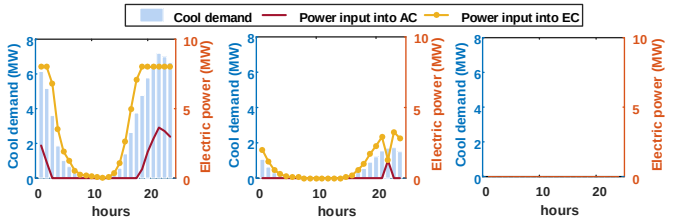

Fig 6 Cooling energy balance

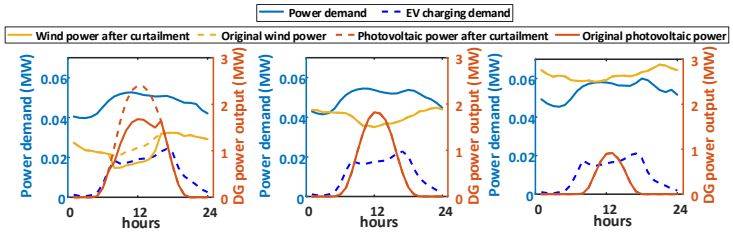

Fig 7 Electrical power balance

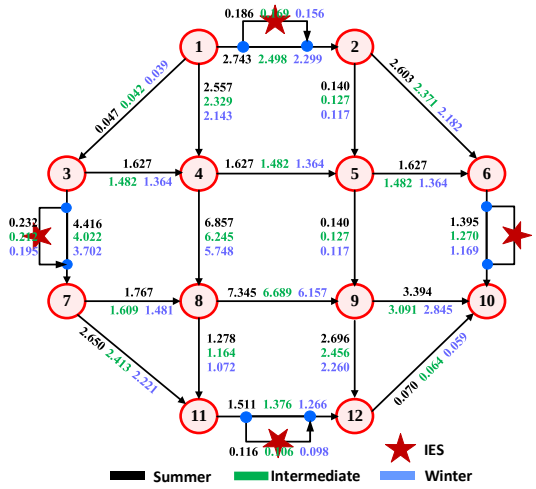

Fig 8 The UE patterns at 18:00 in three typical days.

The mixed UE patterns at evening rush hour (18:00) in three typical days are depicted in Fig 8, showing that the driving patterns in three scenarios obtain a roughly similar UE sate (with only a small numerical difference). This is mainly due to the same O-D pairs. As for the charging route, EVs are recharged mainly in Station 1, 2 and 4 since the route passing station 3 is time-consuming for the EV drivers.

5. CONLUSION

This paper presents an operation framework for urban multi-energy systems considering the charging routes in transportation network. As a basic version, we incorporate the driving patterns by using a mixed user equilibrium for vehicles with and without charging need. The simulation results show that the proposed model can optimize the operation strategies of multiple energy in the integrated energy station effectively. The higher operation cost indicates the importance of the energy conversion. Furthermore, the results of the traffic user equilibrium imply that both vehicles are well-distributed, which is suitable to describe the traffic flow tendency in current smart city.

ACKNOWLEDGEMENT

This work was supported by Science and Technology Project of Fujian Electric Power Co., Ltd (No. 5213001800LH).

REFERENCE

[1] Wang J, Hu Z, Xie S. Expansion planning model of multi-energy system with the integration of active distribution network. Applied Energy. 2019;253:113517.

[2] Wang D, Zhi Y-q, Jia H-j, Hou K, Zhang S-x, Du W, et al. Optimal scheduling strategy of district integrated heat and power system with wind power and multiple energy stations considering thermal inertia of buildings under different heating regulation modes. Applied Energy. 2019;240:341-58.

[3] Wei W, Mei S, Wu L, Shahidehpour M, Fang Y. Optimal Traffic-Power Flow in Urban Electrified Transportation Networks. IEEE Transactions on Smart Grid. 2017;8:84-95.

[4] Zhu J, Yuan Y, Wang W. Multi-stage active management of renewable-rich power distribution network to promote the renewable energy consumption and mitigate the system uncertainty. International Journal of Electrical Power & Energy Systems. 2019;111:436-46.

[5] Yu W, Gong J, Song S, Huang W, Li Y, Zhang J, et al. Gas supply reliability analysis of a natural gas pipeline system considering the effects of underground gas storages. Applied Energy. 2019;252:113418.

[6] Jadidbonab M, Vahid-Pakdel MJ, Seyedi H, Mohammadi-ivatloo B. Stochastic assessment and enhancement of voltage stability in multi carrier energy systems considering wind power. International Journal of Electrical Power & Energy Systems. 2019;106:572-84.

[7] Wei W, Wu L, Wang J, Mei S. Network Equilibrium of Coupled Transportation and Power Distribution Systems. IEEE Transactions on Smart Grid. 2018;9:6764-79.

[8] Xie S, Hu Z, Yang L, Wang J. Expansion planning of active distribution system considering multiple active network managements and the optimal load-shedding direction. International Journal of Electrical Power & Energy Systems. 2020;115:105451.

[9] Xie S, Hu Z, Zhou D, Li Y, Kong S, Lin W, et al. Multi-objective active distribution networks expansion planning by scenario-based stochastic programming considering uncertain and random weight of network. Applied Energy. 2018;219:207-25.